Bulg. J. Phys. **44** (2017) 498–508

$j-1$ Anomaly through the Silver Isotopic Chain

S. Lalkovski
Department of Nuclear Engineering, Faculty of Physics,
St. Kl. Ohridski University of Sofia, 1164, Sofia, Bulgaria

Received *13 November 2017*

Abstract. The silver nuclei are placed in the verge between the classical shell model and collective nuclear regions. As such, properties often attributed to one or another mode are observed to co-exist at low excitation energies. Of particular interest is the competition between the $\pi g_{9/2}^{-3}$ configuration and the core excitations, which has been challenging for a number of theoretical models to describe.
This work presents a systematical study of low-lying excited states in the silver nuclei. A correlation between the $(j, j-1)$ energy gap and the core's 2^+ level energy is observed, which seems to be coherent, to certain extent, with both the particle-core coupling and the shell model approaches.

1 Introduction

The Nuclear Shell model [1] was introduced in the mid 20th century and become one of the cornerstones in the contemporary nuclear physics owing to its success, among others, in describing the nuclear "magic" numbers. It is now well established that these magic numbers emerge due to the spin-orbit force [2, 3] which, at the medium-mass and heavy nuclei, decouples single-particle orbits from the upper shells and pushes them down in energy to the shells where the majority of the single-particle states have parities opposite to that of the "intruder" states. This phenomenon is responsible for the magic gaps formation at occupation numbers 28, 50, 82 and 126, but also for the emergence of some sub-shell gaps, at Z=40 for example, where extra stability towards nuclear excitations is observed. The respective single-particle orbits that take part in the shells re-arrangement are $f_{7/2}$, $g_{9/2}$, $h_{11/2}$ and $i_{13/2}$.

It worth noting that the Nuclear shell model has been developed and parametrized with respect to the nuclei placed on, or close, to the line of β stability. Some recent experiments, however, suggest that the spin-orbit interaction might weaken, or even vanish, in the regions away of that line.

However, already at the line of β stability, the spin-orbit interaction strength varies from shell to shell, and differs for protons and neutrons. The net result

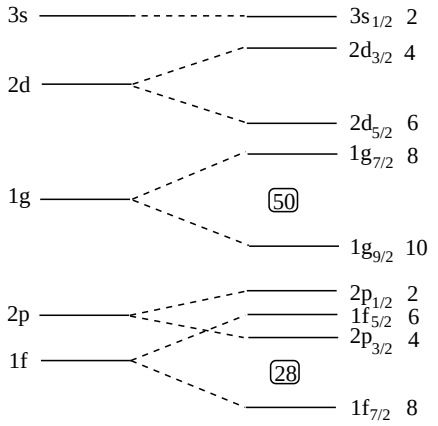

Figure 1. Shell model single-particle states around Z=50, reproduced from ref. [4]

is a slightly different ordering of the single particle levels [3], depending on the mass region and the type of nucleons considered. Figure 1 shows a snapshot of the proton single particle ordering for $A \approx 100$ nuclei, reproduced from Ref. [4]. Given that $\pi g_{9/2}$ is the only positive-parity orbit below the Z=50 magic number, and that it is also responsible for the appearance of the sub-shell closure at Z=40, it is natural to expect that this particular orbit plays a major role in the wave-functions of the positive-parity low-ling states in the Ag nuclei. Indeed, as shown in Figure 2, the lowest-lying positive-parity state observed in $^{97}_{47}\mathrm{Ag}_{50}$ is $9/2^+$, which can be associated with $\pi g_{9/2}$ occupation. The next excited positive-parity state is $7/2^+$, which to certain extent fits to single-particle picture, given

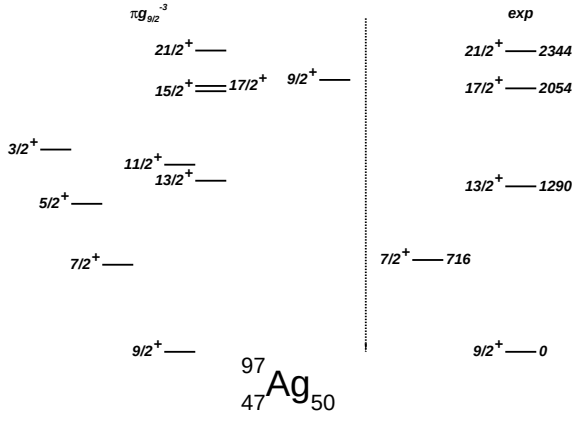

Figure 2. ^{97}Ag level scheme: (left) $\pi g_{9/2}^{-3}$ spectrum; (right) experimental level energies.

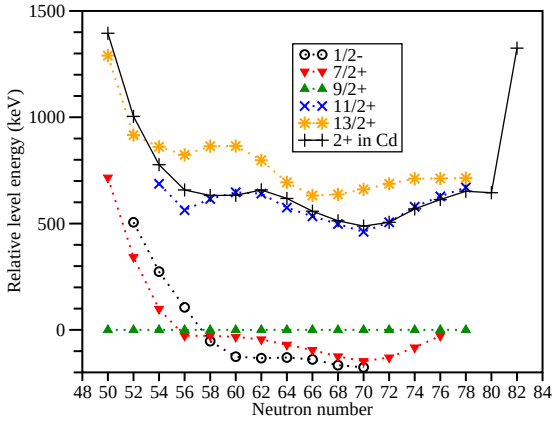

Figure 3. (color online) Yrast states in Ag nuclei as a function of the neutron number. All level energies are relative to the $9/2^+$ level. Modified from [10], including new data from [11] and [12].

that it could arise from excitations across the Z=50 shell gap, and hence can be associated with an occupation of the $\pi g_{7/2}$ orbit. However, the shell gap at Z=50 is about 4 MeV wide. In contrast, the experimental $7/2^+$ state appears to be too low in energy. In the medium-mass silver nuclei the ordering of these two levels is even more tantalizing. There, as shown in Figure 3, $7/2^+$ becomes the lowest-lying positive-parity state. This effect is now known as the $j-1$ anomaly.

2 j^{-3} Coupling Scheme

The idea of $7/2^+$ being a single-particle excitation was abandoned as early, as in the 1960s. At that time the experimental level energies of ^{97}Ag were unknown, since it is the most exotic neutron deficient silver nucleus produced only recently, but the $j-1$ anomaly was already observed throughout the entire silver isotopic chain. In the 1960s, Kisslinger pointed out [5] that in such nuclei the anomalous ordering of j and $j-1$ levels can be generated by three particle/hole single-j clusters. The j^{-3} scheme is a direct derivative from the Nuclear shell model. The excitation spectrum is generated by the residual interaction between the valence protons. Depending on the particular single-particle orbit different spin range can be achieved. In the case of $g_{9/2}^{-3}$ configuration, it consists of a number of states with $J^\pi = 3/2^+$ to $21/2^+$ all of which, except for the first $9/2^+$ state, have a seniority quantum number $v = 3$ [7]. The sole $v = 1$ state is the lowest-lying $9/2_1^+$ state. The j^{-3} level energies [4] are then given by

$$< j^3\alpha; JM|H|j^3\alpha; JM >= 3\sum_{J'}[j^2(J')jJ|\}j^3J]^2 A_{J'}, \qquad (1)$$

Table 1. Coefficients of fractional parentage for $j = 9/2$ [6,7]

J	v	$J'=0$	$J'=2$	$J'=4$	$J'=6$	$J'=8$
3/2	3	–	–	2.18182	0.81818	–
5/2	3	–	0.83333	0.59091	1.57576	–
7/2	3	–	1.57576	0.41958	0.00606	0.99860
9/2	1	0.8	0.25	0.45	0.65	0.85
9/2	3	–	0.09848	1.28497	1.45606	0.16049
11/2	3	–	0.51515	1.18881	0.33939	0.95664
13/2	3	–	0.90909	0.18881	0.77273	1.12937
15/2	3	–	–	0.3986	1.90909	0.69231
17/2	3	–	–	0.87413	0.51818	1.60769
21/2	3	–	–	–	0.7	2.3

where $A_{J'}$ are the two-body matrix elements and $[j^2(J')jJ|\}j^3J]$ are the coefficients of fractional parentage (cfp). Here j denotes the single-particle total angular momentum; J' is the spin to which two of the particles couple; and J is the total three-particle angular momentum. Table 1 shows the cfp's for three particles on $j = 9/2$ [7]. The theoretical ^{97}Ag spectrum, shown in Figure 2 (left hand side), is obtained by using the Talmi procedure. Within this approach the two-body matrix elements are determined from the neighbouring even-even semi-magic nucleus having two particles/holes to the nearest shell closure. In the ^{97}Ag case this is $^{98}_{48}$Cd$_{50}$ for which $A_{J'} = \{0, 1395, 2082, 2280, 2428\}$ keV. Here, J' denotes the spin of the core since the yrast sequence is assumed to arise from a pure $\pi g_{9/2}^{-2}$ coupling scheme.

Alternatively, the two-body matrix elements $A_{J'}$ can be calculated by using the effective quadrupole-quadrupole $Q \cdot Q$ or surface delta (SDI) interactions [8]. These two interactions lead to two distinctive schemes. The SDI preserves [9] the seniority quantum number v and generates $9/2^+$ as the lowest-lying state. Contrary to it, the $Q \cdot Q$ interaction does not preserve seniority and yields a $7/2^+$ state at energy lower than that of $9/2^+$ state. The experimental data in Figure 3 seems to present a transition between these two regimes. In ^{97}Ag, and the neighbouring two isotopes, the $9/2^+$ state is, indeed, the lowest lying positive-parity state. From ^{103}Ag on, however, the $9/2^+$ and $7/2^+$ states swap their places in a $Q \cdot Q$-like manner. This regime seems to be valid up to ^{125}Ag, where the two states are expected to swap their ordering back and the seniority scheme being restored.

More details on the phenomenological shell model calculations, performed for ^{97}Ag, are presented in Figure 2. The ordering of $9/2^+$ and $7/2^+$ levels, as well as the energy gap, are correctly reproduced. The higher-lying $13/2^+, 17/2^+$ and $21/2^+$ yrast states appear also as they were experimentally observed in Ref. [13]. The $J^\pi = 3/2^+$ and $5/2^+$ states are non-yrast and should appear at higher energies, but they were not observed yet. The $11/2^+$, $15/2^+$ and the $v = 3$,

$9/2_2^+$ states are also unknown. Thus, in order to completely test the seniority scheme in ^{97}Ag more experimental data is needed. Nevertheless, the available data is consistent with the j^{-3} coupling scheme.

Based on the assumption that the seniority scheme, as we know it from ^{97}Ag, is restored at the semi-magic $^{129}_{47}\mathrm{Ag}_{82}$, and by knowing the $^{130}_{48}\mathrm{Cd}_{82}$ level scheme with $A_{J'} = \{0, 1325, 1864, 1992, 2130\}$ keV, the $\pi g_{9/2}^{-3}$ level scheme can be calculated as shown in Figure 4. It has to be noted that ^{129}Ag excited levels were not observed yet and any deviation from the $\pi g_{9/2}^{-3}$ pattern, that would be experimentally detected, would indicate deviation from the $N = 82$ magic number since the seniority scheme is sensitive to the location of the shell gaps.

Similar calculations, to that carried out for ^{97}Ag, were recently carried out [10] for all silver isotopes and were found to be consistent, as shown in Figure 15 of ref. [10], with the experimental data. The ^{99}Ag and ^{101}Ag level schemes resemble the ^{97}Ag level scheme. Then, surprisingly, the calculations carried out for the neutron mid-shell silver nuclei, where the valence space is much larger, involving also a large number of neutrons, reproduces well the overall trend of the levels. The ^{113}Ag, shown in Figure 4, is a good example. The $\pi g_{9/2}^{-3}$ calculations were carried out with a proton-proton interaction obtained from the

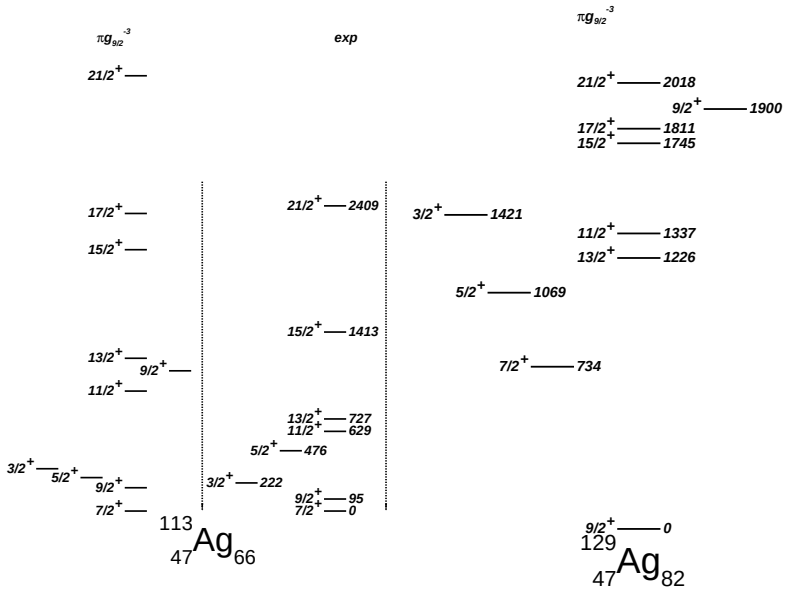

Figure 4. $\pi g_{9/2}^{-3}$ calculations for $^{113}_{47}\mathrm{Ag}_{66}$ and $^{129}_{47}\mathrm{Ag}_{82}$. The neutron mid-shell silver j^{-3} scheme is distinctive and is closer to the experimental data, than the seniority scheme applied for the nuclei near the doubly magic ^{132}Sn and $^{100}_{50}\mathrm{Sn}_{50}$. The $\pi g_{9/2}^{-3}$ calculations performed for $^{97}_{47}\mathrm{Ag}_{50}$ are presented in Figure 2.

neighbouring ^{114}Cd nucleus, for which $A_{J'} = \{0, 558, 1284, 1990, 2669\}$ keV. The ordering of the ^{113}Ag levels is different from that of ^{97}Ag and ^{129}Ag, placed in vicinity to the two doubly magic thin isotopes ^{100}Sn and ^{132}Sn. Indeed, the j^{-3} calculations for ^{113}Ag, and the other neutron mid-shell Ag nuclei, show a level structure similar to that obtained with the $Q \cdot Q$ interaction. It should be noted, however, that these calculations smear the effect of the neutron component through the two-body terms calculated from the neighbouring cadmium nuclei. Another downside of this approach is its incapability to explain the $M1$ transitions observed between the members of the same j^{-3} multiplet [7]. As a consequence, large-space Shell model calculations were carried out for $^{123-129}$Ag [10]. They were performed by taking into account both the proton $\pi 1f_{5/2}$, $\pi 2p_{3/2}$, $\pi 2p_{1/2}$, $\pi 1g_{9/2}$ and the neutron $\nu 1g_{7/2}$, $\nu 2d_{5/2}$, $\nu 2d_{3/2}$, $\nu 3s_{1/2}$, and $\nu 1h_{11/2}$ single-particle orbits. The modern jj45pna effective interaction, parametrized with respect to the A=132 nuclei, was used. As a result, more complex wave function were obtained, but the overall result was worse than that obtained from the three-single-j particles calculations. Nevertheless, these calculations had also shown that the $\pi g_{9/2}^{-3}$ configuration plays an important role in the formation of the positive-parity states in the silver nuclei away from the magic numbers.

Recently, truncated large-scale shell model calculations were performed and compared to two-orbit shell model calculations, where only $\pi g_{9/2}^{-3} \otimes \nu h_{11/2}^{m}$ configurations were taken into account [11]. They show a better description of the positive-parity yrast states in ^{113,119,121}Ag isotopes, emphasizing the role of the $\nu h_{11/2}$ intruder orbit in the nature of the positive-parity yrast states in Ag isotopes.

3 Particle(s)-Core Models

A different approach to the problem has been exploited in the 1970s [14], when a model based on interaction between three-particles (or holes)-cluster interaction with a vibrational field was introduced, and used to describe a large set of states. Several single particle orbits were taken into account in these calculations. In that model, the magnitude of the $(j, j-1)$ splitting is strongly dependent on the the cluster-core interaction strength and the $j-1$ anomaly has been found to emerge at large values of the interaction parameter.

Further, in the 1970s, Axially-Symmetric-Rotor-plus-Particle Model and Traixial-Rotor-plus-Particle Model calculations were performed. Examples are presented in Refs [15] and [16]. Within those models, the $j-1$ anomaly is explained via a particle-deformed core interaction and triaxiallity. More recently, the structure of the mid-shell nuclei ^{111,113}Ag was studied within the Interacting Boson-Fermion Model [12].

The underlying success of those collective models lies in the fact that the va-

lence space of the neutron mid-shell silver nuclei is much larger and quadrupole deformation is developed there, which is a prerequisite for success of the models exploiting particle-core coupling schemes. The two approaches, the shell model and the particle(s)-core models, however, give consistent results, given that the core Cd nuclei already contain the $\nu h_{11/2}$ excitations in their 2^+ level.

4 Nuclear Data Systematics

4.1 Static nuclear moments

Indeed, as shown in Table 2, large electric quadrupole moments Q were measured for the $7/2^+$ state in the neutron mid-shell silver nuclei [18]. Moreover, Q increases towards the neutron mid-shell, and in general, is larger than the quadrupole moments measured for the $3/2^+$ ground state in the nearly doubly magic ^{129}Sn and ^{131}Sn nuclei [18], where $Q = -0.04$ (9) and +0.05 (12) b, respectively. Somewhat controversial is the fact that the electric quadrupole moment of the core cadmium nuclei is of the same magnitude, but of different sign. The same is valid for the palladium nuclei with A=104-110, for which $Q \approx -0.4$ b. There is no enough data for the silver isotope to study the quadrupole deformation evolution in the entire silver isotopic chain, but from the available data a gradual increase towards the neutron mid-shell can be expected for the $7/2^+$ state. Moreover, the magnitude of the quadrupole moment is similar to that, observed for the $7/2^+$ state in the N=60 and 62 isotones, shown in Table 3.

The magnetic moments μ of the $7/2^+$ state, measured only for some of the silver isotopes Table 2, also coincide with the moments, measured in the In and Rh isotones, in Table 3, suggesting that the same state is, indeed, involved in these excitations. But this would be also the case, if the states arise from the single-j, for In isotopes, and the same-j^{-3} coupling scheme, for Ag and Rh

Table 2. Magnetic μ and quadrupole Q moments measured for the Ag nuclei. μ data is taken from [17] and the quadrupole moments are from the most recent compilation [18].

	^{101}Ag	^{103}Ag	^{105}Ag	^{107}Ag	^{109}Ag
J^π	$9/2^+$	$7/2^+$	$7/2^+$	$7/2^+$	$7/2^+$
Q (b)	+0.35 (5)	+0.84 (9)	+0.85 (11)	0.98 (11)	(+)1.02 (12)
μ			+4.414 (13)	+4.398 (5)	+4.400 (6)

Table 3. Magnetic and quadrupole moments in some In, Ag and Rh isotones [17].

	^{109}In	^{111}In	^{107}Ag	^{109}Ag	^{105}Rh
$\mu(7/2^+)$	+5.538 (4)	+5.503 (7)	(+)4.398 (5)	+4.400 (6)	4.4512 (10)
$Q(7/2^+)$	+0.841	+0.804 (22)	0.98 (11)	(+)1.01 (12)	

isotopes. Thus, it is difficult to disentangle the excitation mode based on the magnetic moments data only.

4.2 Reduced transition probabilities

The key experimental evidence in favour of one or the other excitation mode seems to be the electromagnetic reduced transition probabilities for transitions that are expected to connect states from the same "multiplet". Unfortunately, these are scarcely measured too. In fact, there are lifetime data only for few states in $^{105-111}$Ag. In addition, such a study is hindered by the lack of precise mixing ratio measurements, which is a key component in the matrix element calculations. Hence, further experimental measurements are needed in order to obtain a more detailed picture of the structural evolution in the silver isotopic chain.

4.3 Level energy systematics

The systematics of the low-lying positive-parity states in the Ag isotopic chain, presented in Figure 3, shows two overall distinctive regimes. In the light nuclei, placed close to the N=50 magic number, $7/2^+$ appears above the $9/2^+$ state. There, the respective core energy is ≈ 1000 keV. When approaching the neutron mid shell, however, the core 2^+ level energy decreases to 300-600 keV. As a result, the $9/2^+$ and $7/2^+$ states swap their places, and $7/2^+$ becomes the

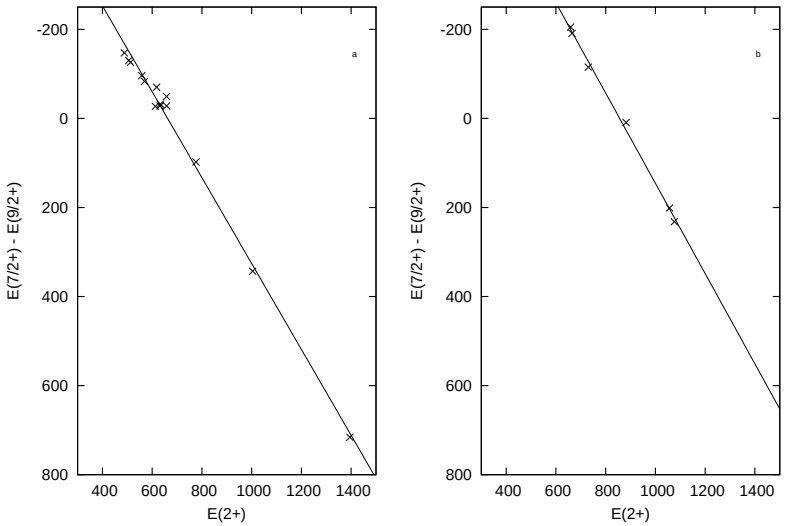

Figure 5. Evolution of the $E(9/2^+) - E(7/2^+)$ energy gap as a function of the core $E(2^+)$ in the Z=47 (left) and N=47 (right) chains.

Table 4. Level energies in Z=47 (Ag) isotopes, compared to E_{2^+} in even-even Z=48 (Cd) and Z=46 (Pd) nuclei. With few exceptions, all energies, in keV, are taken from ref. [19] as of 11.10.2017. The level energies of ^{97}Ag are from [20], those of ^{117}Ag – are from [21]. The level energies for ^{119}Ag are taken from [11] and [22]. ^{121}Ag data is from [11].

N	Ag $E_{9/2^+}$	Ag $E_{7/2^+}$	Ag ΔE	Cd E_{2^+}	N	Ag $E_{9/2^+}$	Ag $E_{7/2^+}$	Ag ΔE	Cd E_{2^+}
50	0	716	716	1395	64	130	60	-70	618
52	0	343	343	1004	66	139	43	-95	558
54	0	98	98	776	68	167	41	-126	513
56	28	0	-28	658	70	176	29	-147	488
58	53	25	-28	632	72	129+x	0+x	-129	506
60	126	93	-33	633	74	83	0	-83	569
62	133	88	-45	658	76	27	0	-27	613

lowest-lying positive parity state in the silver odd mass nuclei. Thus, the position and the ordering of the $7/2^+$ and $9/2^+$ states are strongly correlated with the 2^+ level energy of the core. This is even more prominent in Figure 5 where, on the left hand side, the $\Delta E = E_{7/2^+} - E_{9/2^+}$ level energy difference is plotted as a function of the core's E_{2^+}. A similar study was performed for the N=47 isotones and was found to follow the same trend.

In the $N = 47$ isotonic chain, at low energies, the level schemes are also dominated by positive-parity states arising from $\nu g_{9/2}$ intruder orbit. Again, when the proton number is close to Z=50, the $9/2^+$ level is the lowest-lying positive-parity state. In those nuclei the $7/2^+$ state is lying at higher energies. The precise $9/2^+$ and $7/2^+$ level energies are listed in Table 5 and compared to the 2^+ level energies of the N=48 nuclei. Deeper in the proton shell, when the deformation start to emerge, the two levels swap their places as it is in the Z=47 case.

Thus, at first glance, depending on the relative position with respect to the shell

Table 5. $7/2^+$ and $9/2^+$ level energies in the N=47 isotopes, in keV, compared to the 2^+ level energies in the neigbouring even-even nuclei

Nucleus	$E_{9/2^+}$	$E_{7/2^+}$	ΔE	Nucleus	E_{2^+}
$^{87}_{40}$Zr$_{47}$	0	201	201	$^{88}_{40}$Zr$_{48}$	1057
$^{85}_{38}$Sr^{47}	0	232	232	$^{86}_{38}$Sr$_{48}$	1076
$^{83}_{36}$Kr^{47}	0	9.4	9.4	$^{84}_{36}$Kr$_{48}$	882
$^{81}_{34}$Se$_{47}$	294	103	-191	$^{82}_{34}$Se$_{48}$	665
$^{79}_{32}$Ge$_{47}$	391	186	-205	$^{80}_{32}$Ge$_{48}$	659
$^{77}_{30}$Zn$_{47}$	115	0	-115	$^{78}_{30}$Zn$_{48}$	730

gaps, two excitation patterns can be distinguished. A j^{-3} seniority scheme that can explain the behavior of the nuclei placed close to the shell edges, and a "seniority-broken" regime represented by a different level ordering. Thus, in the nuclei for which one of the two components (protons or neutrons) is close to the magic number and the other is far away from the nearest shell gap, represent excitation features close to the phenomenological j^{-3} configuration with $Q \cdot Q$ interaction, and/or collective-particle(s) model description. The experimental data shown in Figure 3, however, seems to support a more gradual change between these two "orthogonal" regimes.

Nevertheless, what emerges from the systematics in the present study is that the $j, j-1$ splitting strongly depends on the core's 2^+ level energy, suggesting that the core excitation plays an important role already at low excitation energies throughout the entire silver isotopic chain. Similar trend is also observed for the nuclei with three neutron holes below N=50.

5 Conclusion

The Nuclear Shell model and the Particle-Core models are among the cornerstones in the modern Nuclear physics. Their success is based on the applicability of the adiabatic principle which allows to disentangle single-particle from collective modes. Thus, nuclei of well pronounced shell-model behaviour are located near the magic numbers, while nuclei with a large number of valence particles form the regions of collectivity on the Segré chart. In each of these regimes, however, there are distinctive features that are outside the respective model valence space, but rather reside in the "adversary" group of models. Such a feature is the seniority concept, which is well within the spherical shell model space, but it is completely "orthogonal" to the deformed shell model concept. The data, however, seems to support a gradual evolution between the two regimes, that can be tracked by using the low-lying yrast states in the three-holes isotopic and isotonic chains, respectively.

Acknowledgements

This study is supported by the Bulgarian National Science Fund under contract DFNI-E02/6. SL acknowledges interesting discussions with P. Van Isacker.

References

[1] M.G. Mayer (1948) *Phys. Rev.* **74** 235.
[2] O. Haxel, J.H.D. Jensen, H.E. Suess (1949) *Phys. Rev.* **75** 1766.
[3] M.G. Mayer (1950) *Phys. Rev.* **78** 16.
[4] K.L.G. Heyde (1994) "*The Nuclear Shell model*" (Springer-Verlag).
[5] L.S. Kisslinger (1966) *Nucl. Phys.* **78** 341.

[6] I.M. Band, and Yu.I. Kharitonov (1971) *Nuclear Data Tables* **10** 107.
[7] P. Van Isacker, private communications.
[8] A. Escuderos, and L. Zamick (2006) *Phys. Rev. C* **73** 044302.
[9] P. Van Isacker, and S. Heinze (2014) *Ann. Phys.* **349** 73.
[10] S. Lalkovski *et al.* (2013) *Phys. Rev. C* **87** 034308.
[11] Y.H. Kim *et al.* (2017) *Phys. Lett. B* **772** 403.
[12] S. Lalkovski *et al.* (2017) *Phys. Rev. C* **96** 044328.
[13] M. Lipoglavsek *et al.* (2005) *Phys. Rev. C* **72** 061304(R).
[14] V. Paar (1973) *Nucl. Phys. A* **211** 29.
[15] V. Popli *et al.* (1979) *Phys. Rev. C* **20** 1350.
[16] A.W.B. Kolshoven *et al.* (1979) *Nucl. Phys. A* **315** 334.
[17] N.J. Stone (2014) "*Table of Nuclear Magnetic Dipole and Electric Quadrupole Moments*" (INDC(NDS)-0658).
[18] N.J. Stone (2016) *Nucl. Data and Nuclear Data Tables* **111** 1.
[19] ENSDF as of 04/10/2017.
[20] G. Lorusso *at al.* (2012) *Phys. Rev. C* **86** 014313.
[21] J.K. Hwang *at al.* (2002) *Phys. Rev. C* **65** 054314.
[22] E.H. Wang *at al.* (2017) *Phys. Rev. C* **95** 064311.